J. H. FAUPEL and D. B. HARRIS

Engineering Research Laboratory, Engineering Department, E. I. du Pont de Nemours & Co., Inc., Wilmington, Del.

Stress Concentration in Heavy-Walled Cylindrical Pressure Vessels

Effect of Elliptic and Circular Side Holes

Experimental as well as theoretical information is given, in a field where most designers have had to make hopeful guesses

SINCE 1947 the Engineering Research Laboratory of the Du Pont company has been studying the mechanical behavior of materials and equipment under high pressure. A recently published article (*2*) on the behavior of heavy-walled cylinders under internal pressure contains design equations which predict the yield and bursting pressures of both plain and prestressed cylinders. The present article considers the effect of adding either elliptic or circular side holes to heavy-walled cylinders subjected to internal pressures (Figure 1).

A knowledge of the stresses at the cylinder bore–side hole interface is important, because many heavy-walled vessels contain oil holes for lubrication and ports for valves. In particular, for high-pressure applications, a realistic picture of the state of stress in a vessel with side ports is needed because fatigue life is very critical and present-day limitations of strength and ductility in commercial pressure vessel materials prevent high factors of safety. The information given here adds to knowledge of the behavior of vessels at high pressure; future revisions of pressure vessel codes may take advantage of these data. In work on thin-walled vessels (*1*, *6*), bending stresses induced by branch pipes and cover plates are considered. For heavy-walled vessels, two discussions (*3*, *4*) have considered briefly the stress concentration effect of a single circular side hole, but analytical procedures covering the general case (elliptic holes) or the case of cross-bore side holes have not been offered.

Analytical Procedure

In analyzing the state of stress in a cylinder containing side holes it is assumed that analyses established for holes in infinite elastic plates subjected to uniaxial or biaxial stresses can be used. For example, Figure 2 shows an elliptic hole in an infinite elastic plate subjected to tensile loading. For this case Wang has established (*8*), using conformal transformation, that

$$\sigma_x + \sigma_y = S[1 - m^2 - 2\cos 2(\beta - \theta) + 2m\cos 2\theta\cos 2(\beta - \theta) - 2m\sin 2\theta\sin 2(\beta - \theta)]/(1 + m^2 - 2m\cos 2\theta) \quad (1)$$

where

σ_x, σ_y = stresses in the X and Y cartesian directions
S = unit stress
m = $(a - b)/(a + b)$
a = semimajor axis of ellipse
b = semiminor axis of ellipse
β = angle between applied load direction and major axis
θ = angle defining any point on perimeter of ellipse with respect to major axis

When the loading direction is along the X axis ($\beta = 0$), the stresses at the ends of the ellipse axes are found as follows: At the ends of the minor axis $\theta = \pi/2$, $\sigma_y = 0$, and from Equation 1

$$\sigma_x = S_x\,[1 + 2\,b/a] \quad (2)$$

At the ends of the major axis, σ_x, β, and θ are all equal to zero and by Equation 1

$$\sigma_y = -S_x \quad (3)$$

When the loading is along the Y axis, the stress at the ends of the minor axis is found by letting β and θ equal $\pi/2$, with σ_y equal to zero in Equation 1; thus

$$\sigma_x = -S_y \quad (4)$$

and at the ends of the major axis, σ_x and θ equal zero and β equals $\pi/2$ in Equation 1; thus

$$\sigma_y = S_y\,[1 + 2\,a/b] \quad (5)$$

Thus, with appropriate values of σ_x, σ_y, β, and θ substituted in Equation 1, the state of stress for any biaxial loading condition can be determined for any point on the perimeter of the ellipse. Equation 1, for an elliptic hole in an infinite plate represents the general case; the circular hole is a special case of an ellipse with equal axes. Therefore, if the state of stress is required for a circular hole in a plate under uniaxial or biaxial loading, Equation 1 is modified by letting $a = b$. For a circular hole in a plate under uniaxial load, σ_x and σ_y in Equations 2 and 5 become equal to $3S_x$ and $3S_y$, respectively—or, a stress concentration factor of 3 is obtained. If the hole is not small with respect to the plate dimensions, other modifications are required; this is discussed later when the analysis is applied to the case of a side hole in a circular cylinder.

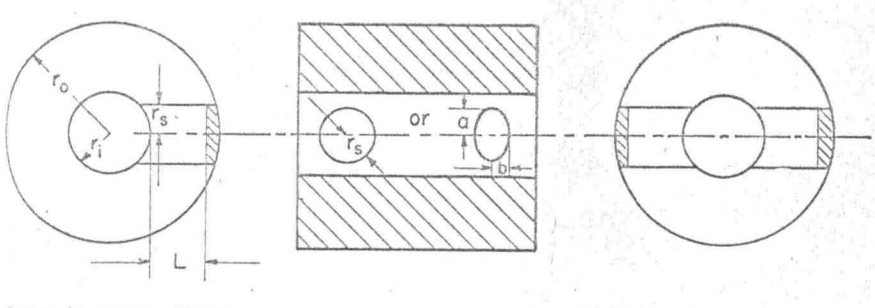

Figure 1. Geometry of side holes in cylinder

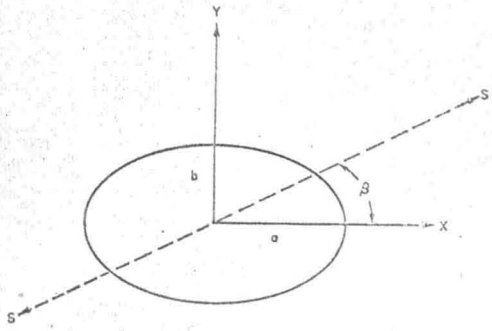

Figure 2. Elliptic hole subjected to unit stress S

Side Holes in Cylinders. The present discussion is concerned only with the stress concentration induced in a cylinder under internal pressure by the presence of circular side holes and elliptic side holes, in which the major axis of the ellipse is perpendicular to the longitudinal axis of the cylinder (Figure 1).

In trying to arrive at theoretical values of stress concentration factors at the bore–side hole interface, the first thought is to treat the cylinder bore like a plate with a hole (Equation 1). When the hole also has pressure in it, one would intuitively expect K factors (stress concentration factors) in excess of 3 and possibly reaching values as high as 5 or 6. Experimental data and theoretical analysis do not support this type of reasoning. In the following analysis the plate theory above is used; first, however, it is necessary to determine how to apply plate theory in the case of a circular cylinder. The distribution of stress in a cylinder containing side holes, where both cylinder bore and side holes are subjected to internal pressure, is complex and thus it is necessary to reduce the situation to a simpler one that is amenable to exact analysis. This is accomplished by noting that the addition of a hydrostatic stress on a system does not alter its fundamental behavior.

Figure 3 shows a closed-end cylinder containing an elliptic side hole subjected to internal pressure; to this picture hydrostatic tension (Figure 4) equal in magnitude to the internal pressure is added. Superposition then gives the situation shown in Figure 5, which is amenable to exact analysis by Lamé's equations for a cylinder subjected to external pressure. Thus, for the cylinder in Figure 5

$$\sigma_h = \frac{p_o r_o^2}{r_o^2 - r_i^2}\left(1 + \frac{r_i^2}{r^2}\right) \qquad (6)$$

$$\sigma_r = \frac{p_o r_o^2}{r_o^2 - r_i^2}\left(1 - \frac{r_i^2}{r^2}\right) \qquad (7)$$

$$\sigma_z = \frac{p_o r_o^2}{r_o^2 - r_i^2} \qquad (8)$$

where

$\sigma_h, \sigma_r, \sigma_z$ = circumferential, radial, and longitudinal stresses in cylinder
p_o = external pressure
r_i, r_o = inside and outside radii of cylinder
r = variable radius in cylinder

The location of maximum stress concentration is at A on the bore surface, Figure 5; therefore, in Equations 6 and 7, $r = r_i$ and

$$\sigma_{h(\max)} = \frac{2p_o R^2}{R^2 - 1} \qquad (9)$$

$$\sigma_r = 0 \qquad (10)$$

$$\sigma_z = \frac{p_o R^2}{R^2 - 1} \qquad (11)$$

where $R = r_o/r_i$

Elastic plate analysis can now be applied to the cylinder problem. The hoop stress generated at the bore of the cylinder (Equation 9) is interpreted as the unit stress, S_x, in Equation 2; thus

$$\sigma_x = \frac{2p_o R^2}{R^2 - 1}\left(1 + 2\frac{b}{a}\right) \qquad (12)$$

Because the cylinder has closed ends, a longitudinal stress is generated (Equation 11) which is interpreted as unit stress S_y in Equation 4, so that

$$\sigma_x = \frac{p_o R^2}{R^2 - 1} \qquad (13)$$

Stresses σ_x given by Equations 12 and 13 are both generated at location A, Figure 5, and are additive; thus, the total effective hoop stress in the cylinder at A is as follows:

$$(\sigma_h)_A = \frac{2p_o R^2}{R^2 - 1}\left(1 + 2\frac{b}{a}\right) - \frac{p_o R^2}{R^2 - 1} \qquad (14)$$

The normal hoop stress at A is given in Equation 9; therefore, at this location the stress concentration factor, K, is

$$K = \frac{\frac{p_o R^2}{R^2 - 1}(1 + 4\,b/a)}{\frac{2p_o R^2}{R^2 - 1}} = \frac{1 + 4\,b/a}{2} \qquad (15)$$

Use of Equation 15 now permits the calculation of specific stress-concentration factors depending on the geometry of the side holes. If the side hole is small and circular, $a = b$ in Equation 15 and $K = 2.5$. For an elliptic hole of geometry $a/b = 2$, $K = 1.50$. These K values indicate the influence of the longitudinal stress in a cylinder on stress concentration at side holes—for example, with no longitudinal stress and a circular side hole K would be 3.0, the same as in a plate under tension—the presence of the longitudinal stress decreases this value to 2.5, or a decrease of 16.7%.

The K factor is determined after the application of hydrostatic tension to the cylinder (Figure 5). Therefore, in using the above theory to solve practical problems, one must keep this fact in mind and make calculations accordingly. For example, suppose the cylinder has open rather than closed ends; in this case, the effect of superposition of hydrostatic tension would give the result in Figure 5 minus the tensile force distributed over the bore area and the resultant longitudinal stress would be p_o rather than the stress expressed by Equation 11. Thus, in the paragraph above zero longitudinal stress could result only by the application of a compression force to the end of the cylinder, which would be canceled by the hydrostatic tension. For an open-end cylinder the K factor for a small circular hole would be not 3.0 but $3.0 - \left(\frac{R^2 - 1}{2R^2}\right)$; in other words, for an open-end cylinder the K factor depends on the wall ratio, R.

The foregoing portion of the analysis

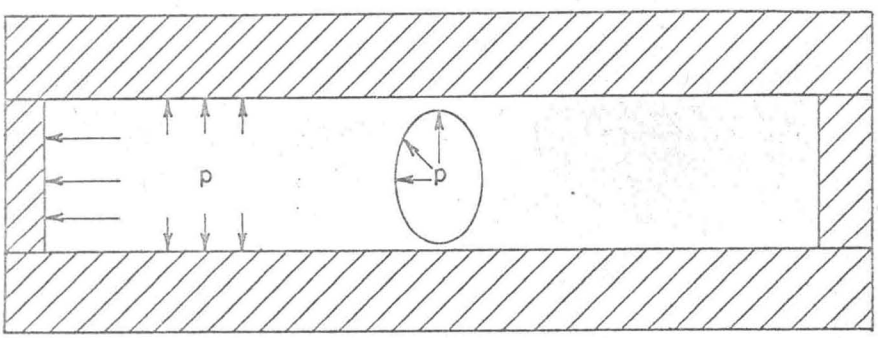

Figure 3. Closed-end cylinder with side hole subjected to internal pressure

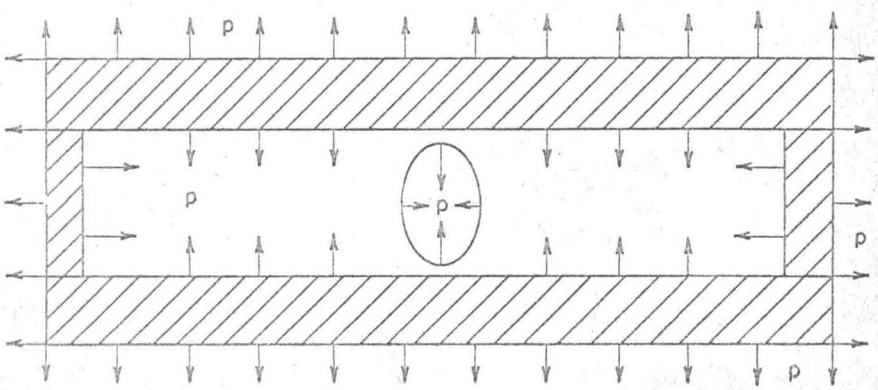

Figure 4. Cylinder subjected to hydrostatic tension

is a basis on which to calculate other values. For example, when the side hole is not small or when there are two side holes diametrically opposed, the intensification factors for small single holes are not valid. To account for the size of the side hole, an expression for the longitudinal stress, σ_z, was developed based on the net section of the cylinder cross section supporting the load; this automatically takes into account the effect of changing the side-hole geometry.

Consider Figure 1 and take the pressure length of the side hole as three fourths of the hole length (this was the case in the experimental work). Thus,

$$L = 3/4\,(r_o - r_i) \qquad (16)$$

Now because stress is equal to load divided by area

$$\sigma_z = \frac{\text{force}}{\text{net area}} = \frac{p_o \pi r_o^2}{\pi(r_o^2 - r_i^2) - 2nr_s L} \qquad (17)$$

where $n = 1$ for one side hole and 2 for the case of two diametrically opposite holes. Thus, from Equation 17, for the case of a single side hole (elliptic or circular)

$$\sigma_z = \frac{p_o \pi R^2 R_s}{(R-1)\,[\pi R_s(R+1) - 1.5]} \qquad (18)$$

and for two diametrically opposite side holes

$$\sigma_z = \frac{p_o \pi R^2 R_s}{(R-1)\,[\pi R_s(R+1) - 3.0]} \qquad (19)$$

where R_s = side hole ratio; r_i/r_s for a circular hole and r_i/a for an elliptic hole.

Case of Circular Side Holes. Equation 17 gives an expression for the longitudinal stress as a function of the geometry of the cylinder. To assign the proper stress intensification values to σ_h and σ_z for calculating the K factor for large side hole sizes, reference is made to the recent compilation of data by Peterson (*5*). Pertinent data from Peterson (Figure 6) come from a consideration of two circular holes in a plate subjected to axial loading. These curves show the effect on stress concentration of the proximity of holes; for a cylinder with two side holes diametrically opposed

Table I. Intensification Factors

Side Hole Ratio, R_s	Factor for σ_h, α	Factor for σ_z, γ
10	3	−0.92
9	3	−0.90
8	3	−0.88
7	2.96	−0.86
6	2.95	−0.84
5	2.92	−0.81
4	2.88	−0.77
3	2.82	−0.70
2	2.71	−0.58
1	2.57	−0.33

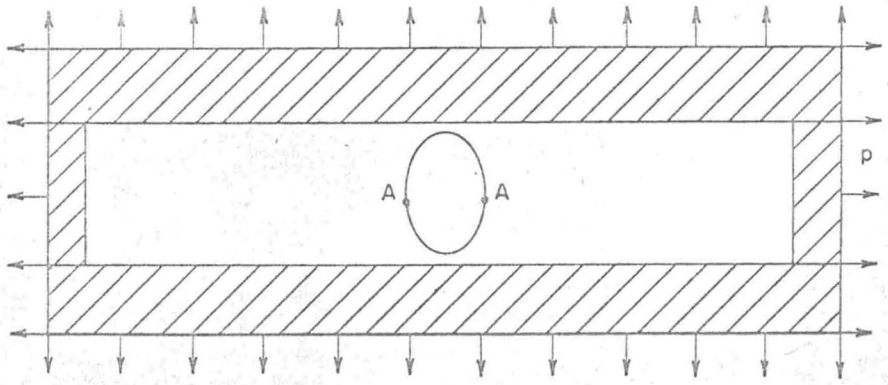

Figure 5. Superposition of Figures 3 and 4

the proximity factor is interpreted as the side hole ratio, r_i/r_s. Curve A of Figure 6 is used to arrive at intensification values for the hoop stress at location A, Figure 5. σ on the plot represents the hoop stress, σ_h, in the cylinder which is intensified to σ_{max} as shown. Thus, for the case of a circular cross-bore side hole, if R_s is equal to 7, σ_h is intensified by a factor equal to about 2.98.

The intensification factors for σ_z are obtained from curve B of Figure 6. For this case σ represents the longitudinal stress, σ_z, in the cylinder with a maximum value, σ_{max}, as shown. This maximum longitudinal stress is positive, but according to plate theory it would induce a negative stress at a location 90° from σ_{max} (the σ_h direction in the cylinder). Thus, as an approximation, if σ_{max} were 3σ, the longitudinal stress would be reflected in the σ_h direction as $-\sigma_z$; if σ_{max} were 1.5 σ, the longitudinal stress would be reflected as 50% of −1.0 or $-0.5\sigma_z$. Thus, from Figure 6, if the side hole ratio were 7, σ_h would be intensified by a factor equal to about 2.98 and to this would be added the effect of the longitudinal stress, $-0.86\ \sigma_z$. Intensification factors for circular side holes have been listed in Table I for a series of cylinders. With these factors the stress-concentration factor, K, for the hoop stress at the bore–side hole interface can be calculated as follows:

$$K = \frac{\alpha\sigma_h + \gamma\sigma_z}{\sigma_h} \qquad (20)$$

where α and γ are intensification factors determined from Figure 6, σ_h is calculated from Equation 9, and σ_z from Equation 17.

Case of Elliptic Side Holes. In analyzing the case of elliptic side holes the procedure used to determine the effect of circular side holes is applied, except

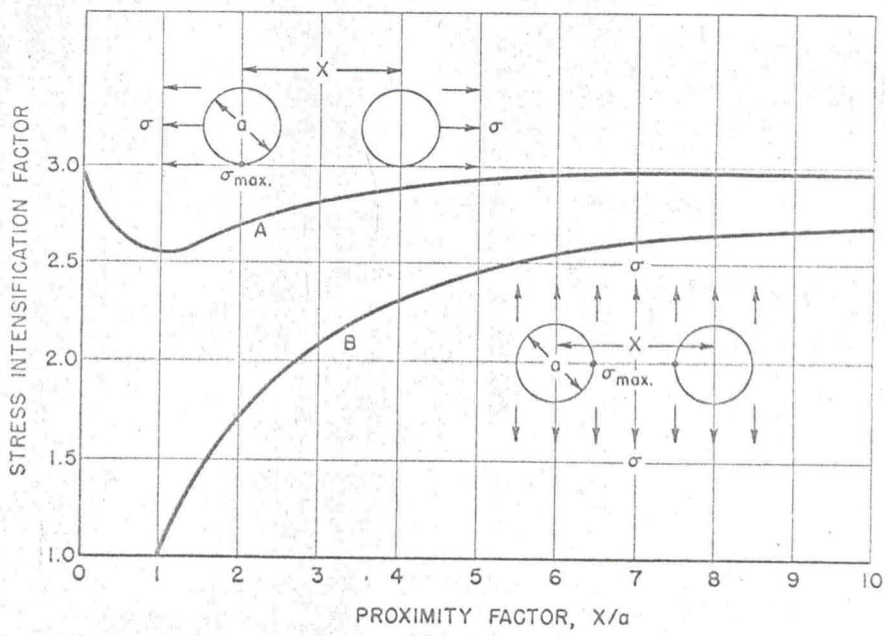

Figure 6. Stress intensification factors

that different intensification factors are applied to σ_h and σ_z. For example, for a circular cylinder having a diameter ratio, r_o/r_i, of 2.5 containing a single elliptic side hole of axis ratio a/b equal to 2.0

$$(\sigma_h)_{max} = \frac{4\,p_o R^2}{R^2 - 1}$$

$$\sigma_z = \frac{p_o \pi R^2 R_s}{(R-1)\,[\pi R_s (R+1) - 1.5]}$$

and

$$K = 2 - \frac{3.5\pi}{2\pi\,(3.5) - 1.5} = 1.46$$

As data are not available for multiple elliptical holes similar to those in Figure 6 for multiple circular holes, this case cannot be analyzed at this time.

Experimental Methods

Two experimental techniques, strain gages and photoelasticity, have been used to determine stress concentrations in cylinders containing side holes or pipe branches. The latter technique has received somewhat more attention than the former; however, so few data have been reported on this problem that the merits of each cannot be evaluated. Naturally, photoelasticity is of great value in solving complex problems, especially where the principal stress directions are not known. On the other hand, the use of strain gages, where applicable, saves considerable time and does not require the specialized knowledge needed for photoelastic work. In this discussion data derived from these two experimental techniques are reported.

Photoelastic Tests. Photoelastic tests, using the frozen stress technique, were performed on cylinders containing circular side holes; only final results are reported here. Two experimental stress concentration measurements were made using circular cylinders having a diameter ratio, r_o/r_i, of 2.5; one cylinder contained a single circular side hole having an R_s of 2.0 and the other cylinder contained a cross-bore circular hole having an R_s of 2.0. One photoelastic test was conducted on a cylinder having an R value of 2.5 and containing a cross-bore slot. The cross-bore slot was made by drilling two circular holes tangent to each other and milling out the central portion, so that the long axis of the slot was perpendicular to the longitudinal axis of the cylinder. The ratio of length to width of the slot was 2.0—this geometry of side hole is thus intermediate between a circular side hole and an elliptic side hole.

Strain Gage Tests. For convenience in mounting strain gages and to eliminate the necessity of making strain measurements under high fluid pressure (as it would be in a metal cylinder), a plastic material was used for the cylinders: An epoxy resin (Ciba Co.'s Araldite 502). The cylinders were cast initially into semicylinders, leaving the bore exposed for easy access. The semicylinders were clamped together to form a cylinder, and circular cross-bore side holes drilled. Initially, two cylinders were fabricated. One cylinder (modulus of elasticity of 355,500 pounds per square inch and Poisson ratio of 0.44) had an R value of 2.0 and an R_s value of 1.0. The other cylinder (modulus of elasticity of 473,000 pounds per square inch and Poisson ratio of 0.37) had an R value of 4.0 and an R_s value of 2.0. This latter cylinder was subsequently reduced, by turning down the outside diameter, to cylinders having R values of 3, 2.5, 2.0, and 1.5; in all cases R_s remained at a constant value of 2.0. Thus one cylinder provided for five tests.

After the circular side holes were bored, the cylinder halves were separated and SR-4 electrical resistance gages (Type 8A-3, 60-ohm, 1/8-inch gage length) were mounted on the main cylinder bore near the side-hole interface, approximately as sketched on Figure 7, by using Type Al Epon strain-gage cement. Five hoop-direction and five longitudinal-direction gages mounted within 1/2 inch from the side hole in each half of the cylinder provided data for stress-concentration calculations. Gages were also mounted 4 to 6 inches from the side hole, where it was felt that stress-concentration effects would be small.

After the gages were cemented in place, the two cylinder halves were cemented together, plugs of the cylinder material were cast into the ends of the cylinder, and provision was made in the

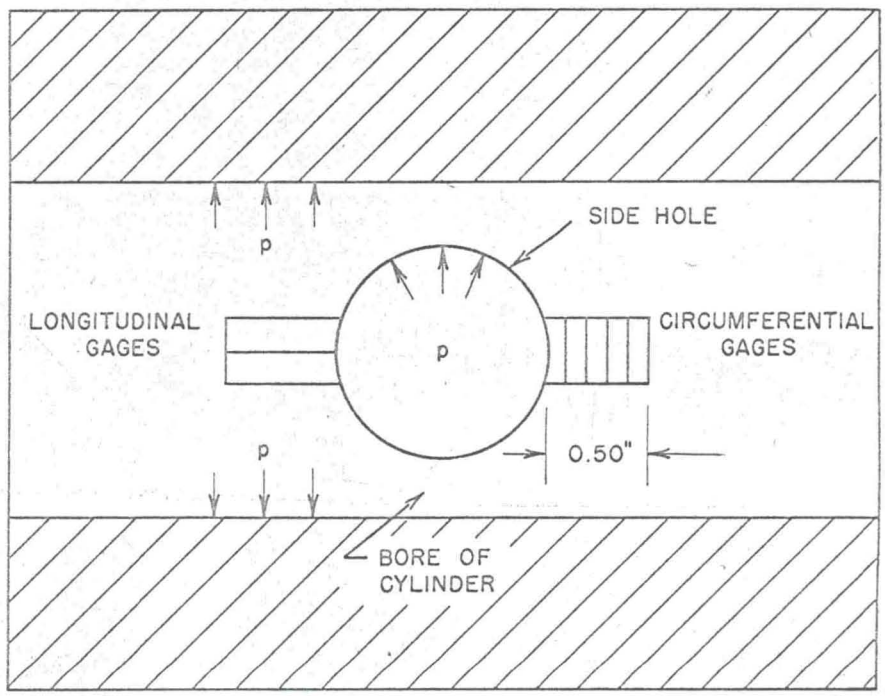

Figure 7. Location of strain gages on bore of cylinder

Table II. Data Used in Calculating Stress Concentrations for Cylinder of Wall Ratio $R = 2$ and Side Hole Ratio $R_s = 1$

Distance from Side Hole, Inches	Strains, Inch/Inch[a] Hoop	Strains, Inch/Inch[a] Longitudinal	Hoop Stress Concn. Factor, K
0	+0.000833	[b]	3.020
0.10	+0.000725	−0.000190	2.820
0.30	+0.000600	−0.000105	2.462
0.50	+0.000528	−0.000065	2.187
0.70	+0.000471	−0.000040	1.927
1.00	+0.000415	−0.000020	1.677
2.00	+0.000310	+0.000020	1.217

[a] For this cylinder E = 355,500 lb./sq. inch., μ = 0.44, o.d. = 3.875 inches, i.d. = 1.9375 inches.

[b] At side hole interface $\sigma_r = \sigma_z = -p$; this information leads to a calculated value of K at interface of 3.020.

side holes to keep the pressurized length about $^3/_4$ $(r_o - r_i)$. The cylinders were then tested by applying up to 50 pounds per square inch internal pressure in 10 pounds per square inch increments by means of a tank of commercial nitrogen. Strains were measured by a Baldwin strain indicator.

Pressurizing the cylinders to 50 pounds per square inch resulted in linear elastic behavior for all gages. The strains measured were averaged for the two halves of the cylinder and these average results were used to calculate the stress-concentration factors (K factors).

Results

The results of the strain gage tests are given in Figure 8 as plots of the stress concentration factor in the hoop direction *vs.* distance along the longitudinal axis of the cylinder from the side hole. For the geometry tested the stress concentration was maximum in the hoop direction of the cylinder at the edge of the side hole and decreased as the distance from the side hole increased. The curve for the cylinder having a wall ratio, $R = 2$, and a side hole ratio, $R_s = 1.0$, was calculated by using the following formula and the strain values listed in Table II.

$$K = \frac{\sigma_h}{(\sigma_h)_n} = \frac{E(\epsilon_h + \mu\epsilon_z) - \mu p(1 + \mu)}{(1 - \mu^2)\, p \left(\frac{R^2 + 1}{R^2 - 1}\right)} \qquad (21)$$

where

E = modulus of elasticity
ϵ_h, ϵ_z = hoop and longitudinal strains, respectively
μ = Poisson's ratio
p = internal pressure
σ_h = hoop stress in cylinder with stress concentration effect
$(\sigma_h)_n$ = normal hoop stress in cylinder

The remainder of the curves on Figure 8 for cylinders having side hole ratios $R_s = 2$, were calculated by using the following formula and the stress and strain values listed in Table III.

$$K = \frac{\sigma_h}{(\sigma_h)_n} = \frac{E\epsilon_h + \mu(\sigma_r + \sigma_z)}{p \left(\frac{R^2 + 1}{R^2 - 1}\right)} \qquad (22)$$

where

σ_r = radial stress $= -p$
σ_z = longitudinal stress

For this group of cylinders ($R_s = 2$), the longitudinal strains were not measured close to the side hole interface; consequently, to calculate K values, the longitudinal stress, σ_z, had to be approximated so that Equation 22 could be used. This was done by superposing two stresses; one stress, σ_z', was the usual longitudinal stress given by the equation

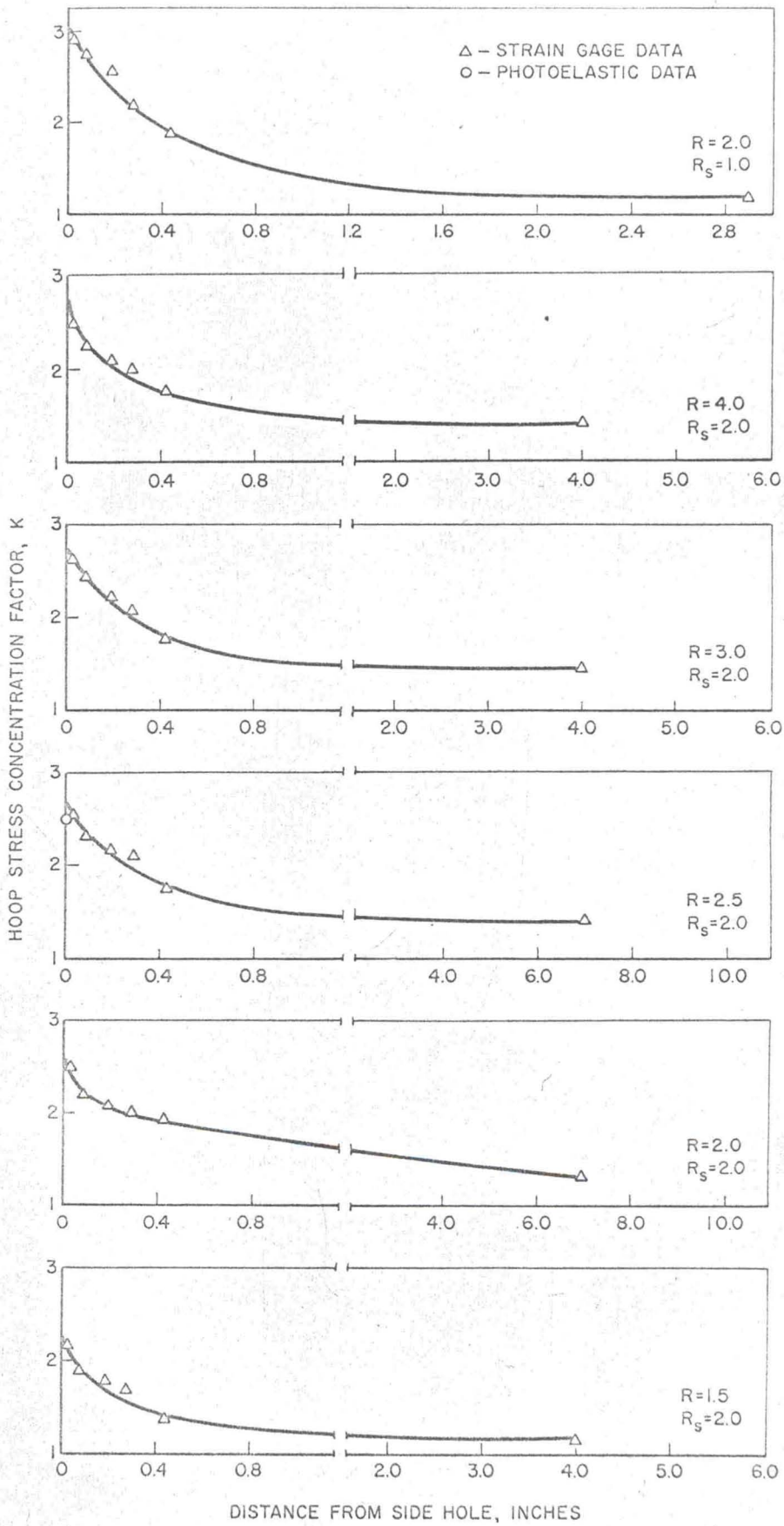

Figure 8. K curves for various cylinders

Table III. Data Used in Calculating Stress Concentrations for Cylinders of Various Wall Ratios with Side Hole Ratio $R_s = 2$

Distance from Side Hole, Inches	Hoop Strain[a], Inch/Inch	Longitudinal Stress, Lb./Sq. Inch	Hoop Stress Concn. Factor, K
	$R = 4.0$ (O.D. = 7.625 Inches)		
0	...	...	2.800[b]
0.05	+0.000367	−93	2.460
0.08	+0.000335	−88	2.230
0.20	+0.000310	−79	2.080
0.28	+0.000296	−74	1.990
0.42	+0.000257	−67	1.700
4.00	+0.000165	+ 3	1.390
	$R = 3.0$ (O.D. = 5.725 Inches)		
0	...	...	2.750[b]
0.05	+0.000417	−90	2.630
0.08	+0.000388	−85	2.440
0.20	+0.000358	−76	2.260
0.28	+0.000335	−71	2.110
0.42	+0.000285	−64	1.780
4.00	+0.000190	+ 6	1.480
	$R = 2.5$ (O.D. = 4.77 Inches)		
0	...	...	2.700[b]
0.05	+0.000441	−86	2.560
0.08	+0.000404	−81	2.340
0.20	+0.000377	−72	2.190
0.28	+0.000361	−67	2.120
0.42	+0.000305	−60	1.770
4.00	+0.000198	+10	1.410
	$R = 2.0$ (O.D. = 3.816 Inches)		
0	...	...	2.620[b]
0.05	+0.000506	−79	2.520
0.08	+0.000450	−74	2.220
0.20	+0.000422	−65	2.100
0.28	+0.000403	−60	2.020
0.42	+0.000338	−53	1.960
4.00	+0.000221	+17	1.340
	$R = 1.5$ (O.D. = 2.862 Inches)		
0	...	...	2.350[b]
0.05	+0.000636	−56	2.160
0.08	+0.000561	−51	1.900
0.20	+0.000522	−42	1.780
0.28	+0.000494	−37	1.700
0.42	+0.000405	−30	1.390
4.00	+0.000284	+40	1.150

[a] For these cylinders E = 473,000 lb./sq. inch and $\mu = 0.37$.
[b] By extrapolation of K curves to side hole interface.

Table IV. Comparison of Stress-Concentration Factors

Diameter Ratio of Cylinder, R	Side Hole Ratio, R_s	Type of Hole[a]	K Factors: Strain gage	K Factors: Photoelastic	K Factors: Theory	Deviation, %
1.5	2.0	CCB	2.350		2.35	0
2.0	1.0	CCB	3.020		2.33	−23
2.0	2.0	CCB	2.620		2.37	−10
2.5	2.0	CCB	2.70		2.38	−12
2.5	2.0	CCB	...	2.40	2.38	−1
3.0	2.0	CCB	2.75		2.38	−13
4.0	2.0	CCB	2.80		2.39	−15
2.5	2.0	SLC	...	1.70	...	...
2.5	2.0	SE	...	...	1.46	...
1.5[b]	8.0	SC	...	(1.70)	2.50	(+47)
				(2.22)		(+13)
2.5	2.0	SC	...	2.35	2.40	+ 2
3.0[c]	2.0	SC	...	2.80	2.40	−14

[a] CCB. Circular cross-bore hole;
SC. Single circular hole.
SLC. Slot cross-bore hole.
SE. Single elliptic hole.
[b] From (4).
[c] From (3).

$$\sigma_z' = \frac{p}{R^2 - 1} \qquad (23)$$

At the side hole interface this stress is zero and rapidly approaches a constant value in accordance with St. Venant's principle (7). The other stress, σ_{zl}, is determined by considering the zone between the side hole and the end of the cylinder as having a stress distribution expressed by the following equation for the radial direction in a cylinder under internal pressure

$$\sigma_{zl} = \frac{p}{(R_1)^2 - 1}\left(1 - \frac{(b_1)^2}{(r_1)^2}\right) \qquad (24)$$

where

R_1 = distance from side hole to end of cylinder divided by side hole radius
b_i = distance from side hole to end of cylinder
r_i = any intermediate distance from side hole to end of cylinder

Analyses of photoelastic data, as well as similar calculations on the cylinder having a side hole ratio $R_s = 1.0$, supported the calculation of the longitudinal stress as outlined above.

In Figure 8 one of the photoelastically determined K factors is plotted and in Table IV the results of all the tests are recorded and compared with theory; this table also includes data from the literature.

Discussion

In Figure 8 the stress-concentration effects are shown to extend beyond the expected limit of perhaps two side-hole diameters. If this condition is fortuitous, and it may be, on the basis of results of photoelastic tests, the actual factors may be somewhat lower than indicated. There are obvious items associated with the strain gage tests which may have had an undue influence on the results. For example, the cement holding the two cylinder halves together could disturb the uniformity of stresses induced by internal pressure. The presence of strain gages cemented to the bore of the cylinders could disrupt the stresses. Finally, for the large side hole size ($R_s = 1.0$) the limitations of the plate theory used in the analytical procedure may have been exceeded; bending stresses, if present, were not included in the analysis. In any event, Figure 9, a summary of the data, indicates an important design item—that as the R value of the cylinder increases, K also increases. From Figure 9, the indication is that K decreases as R_s decreases; however, there may be some question about the K values of $R_s = 1.0$ on the plot. If additional work is undertaken on the problem, K values for $R_s = 1.0$ should be determined.

The photoelastic test results also require some comment. The method is

straightforward; however, precise work is required and exceptional care should be exercised in interpretation of results. In Table IV the two photoelastic test results check theory almost exactly; these tests were conducted and interpreted under most exacting conditions. To avoid the masking effects of stress gradients, compensator readings were taken as successive reduction of specimen thickness and the results were extrapolated to the state of stress at the surface of the bore. It is possible that the two photoelastic test results reported in the literature (R = 1.5 and 3.0) were not based on such a procedure, and this may account for their failure to check theory more closely. In particular, the result for the cylinder of R = 1.5 seems to be too low. On the basis of information given in the reference to this work it is estimated, on the basis of stress gradients, that the true K factor for the cylinder is 2.2, which fits into the over-all picture very well.

The only cylinder with side holes that were not circular contained a slot. This slot approximated an ellipse having an axis ratio a/b of 2.0—it exhibited a K factor at the cylinder bore–side hole interface of about 1.7. The theoretical result for a single elliptic side hole is 1.46. Although in this case the theoretical result for a single elliptic side hole cannot properly be compared with the experimental result for a cross-bore hole that is not a true ellipse, the qualitative check is good. Actually the slot should induce more stress concentration effect than an ellipse, as it is intermediate in geometry between the circle and the ellipse.

An examination of the data in Table IV reveals that the predictions are by no means perfect, although they are probably acceptable from an engineering point of view. Work still remains to be done on this problem.

Application of Theory

Examples given below illustrate use of the theory and its application to engineering design.

Example 1. Design of Plain Monobloc Cylinders with Circular Side Holes. If K values are available, it is possible to estimate the elastic-limit pressure for a cylinder containing side holes. Assuming that the cylinder is initially stress-free, the elastic-limit pressure is obtained by substituting maximum principal stress values for a cylinder, corrected for stress concentration, into the von Mises criterion for failure; thus, for a closed-end cylinder (A, Figure 5)

$$\sigma_{h(\max)} = Kp\left(\frac{R^2+1}{R^2-1}\right) \quad (25)$$

$$\sigma_{r(\max)} = -p \quad (26)$$

and

$$\sigma_{z(\max)} = -p \quad (27)$$

These stresses are related by the von Mises criterion to the yield strength of the material in tension, σ_o, as follows:

$$\sigma_o = (\sigma_h^2 + \sigma_r^2 + \sigma_z^2 - \sigma_h\sigma_r - \sigma_r\sigma_z - \sigma_z\sigma_h)^{1/2} \quad (28)$$

Substitution of Equations 25 to 27 in Equation 28 thus gives an expression for the elastic-limit pressure, p_y, of a cylinder,

$$p_y = \sigma_o(R^2-1)\,[R^4(K^2+2K+1) + 2R^2(K^2-1) + (K^2-2K+1)]^{-1/2} \quad (29)$$

If R = 2 and R_s = 4, from Figure 9, K = 2.47 and by Equation 29

$$p_y = 0.195\,\sigma_o \quad (30)$$

If there were no side hole,

$$p_y = \sigma_o(3)^{-1/2}\left(\frac{R^2-1}{R^2}\right) = 0.432\,\sigma_o \quad (31)$$

For this case the cylinder with the side holes would yield (locally) at a pressure 55% lower than the cylinder without side holes.

If R is increased to 4 in a cylinder with no side holes, then by Equation 31

$$p_y = 0.54\,\sigma_o \quad (32)$$

or an elastic-limit pressure increase of 25% over that obtained for the cylinder with a wall ratio of 2. However, for R = 4 and R_s = 4, K = 2.485, and by Equation 29

$$p_y = 0.258\,\sigma_o \quad (33)$$

or an increase in elastic-limit pressure of about 32%. Thus benefit can be obtained, elastically, in increasing the wall ratio; even though the K values increase with increasing wall ratio, the elastic-limit properties increase at a more rapid rate (due to increase in wall ratio) than the decrease in elastic-limit properties caused by increasing K. For each case, however, the situation should be examined in order that realistic values may be assigned to specific designs.

On the other hand, difficulty could be encountered in a particular case, designed to operate within the elastic range, if additional side holes of different R_s values were used. For example, if R = 2 and R_s = 1, then by Equation 29 and Figure 9

$$p_y = 0.218\,\sigma_o \quad (34)$$

Now if to this cylinder an additional set of side holes is introduced having an R_s value of, say, 10 (small oil hole), then

$$p_y = 0.151\,\sigma_o \quad (35)$$

or a decrease in elastic-limit pressure of 31%.

Example 2. Comparative Design of Cylinders with Circular Side Holes. In this example some comparisons are made relative to the elastic-limit pressures of cylinders of various R values containing circular side holes of various R_s values. The comparison includes a conventional design where the stress concentration factor is assumed to be 6.00.

As in Example 1, Equations 25 to 27 define the state of stress in the cylinders, which when put into Equation 28 gives the elastic-limit pressure defined by Equation 29, where K is determined from Figure 9. The results of some calculations are shown in Table V, where relative elastic limits for cylinders of various geometries are listed. When the side hole ratio, R_s, is infinity it is assumed that the cylinder acts as a plain monobloc with a relative elastic

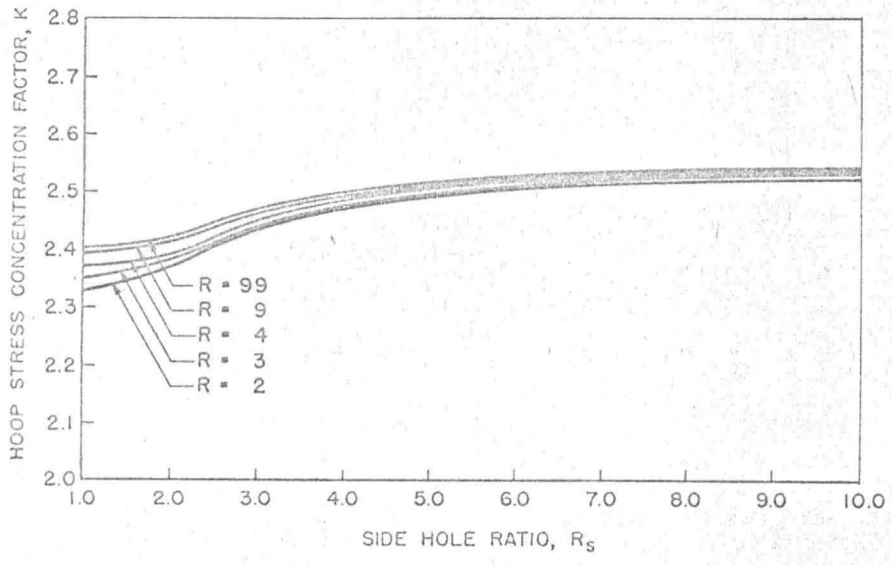

Figure 9. K values for various cylinder geometries

limit of 1.00 for a wall ratio of 2.0 and 1.315 for a cylinder where $R = 9.0$. This is just another way of saying that if the wall ratio of a cylinder is increased from 2 to 9, the elastic-limit pressure increases 31.5%. Furthermore, still referring to Table V, a cylinder having a wall ratio of 9 and a side hole ratio of 5 exhibits an elastic-limit pressure equal to 64.5% of that exhibited by a plain monobloc cylinder having a wall ratio of 2.0.

The real value of having more precise values for stress concentration factors in cylinders with side holes can be illustrated by noting the relative elastic-limit values in Table V corresponding to the last column marked "Variable ($K = 6$)." In many conventional designs it has been customary to use K values as high as 6.0, regardless of the side hole size, simply because the true value has not been known. When such a large factor is used, for example, the calculated elastic-limit pressure for a cylinder having a wall ratio of 4.0 is only 29.6% of that exhibited by a plain monobloc cylinder having a wall ratio of 2.0, regardless of the hole size (R_s value). Now, if R_s is taken into account, Table V shows for the same cylinder having a wall ratio of 4.0, that for an R_s of 5.0, the elastic-limit pressure is 60.5% of that exhibited by the plain monobloc of wall ratio $R = 2.0$. In other words, a factor of about 100% is involved and when the true value of K is used overdesign is avoided. Safety factors are always used; however, if the safety factor is 2, the equipment should be proportioned to give this factor of safety and not a factor of 4, which may occur if the proper values of K are not used.

Example 3. Use of Elliptic Side Holes. When a circular side hole is placed in a cylinder, the maximum stress concentration occurs in the hoop direction at the side hole–bore interface. This K factor can be reduced by making the side hole elliptic in shape; however, it is important not to introduce a K factor at the ends of the major axis of the ellipse which, when applied to the longitudinal stress, would create a situation worse than that obtained in the hoop direction for a circular side hole.

The limiting case for a single small elliptic side hole will now be considered for cylinders with both open and closed ends. In the closed-end cylinder, the total effective hoop stress at the ends of the minor ellipse axis is given by the sum of Equations 2 and 4,

$$\sigma_h = \frac{2p_oR^2}{R^2 - 1}(1 + 2\,b/a) - \frac{p_oR^2}{R^2 - 1} \quad (36)$$

The total effective longitudinal stress at the ends of the major ellipse axis is given by the sum of Equations 3 and 5,

$$\sigma_z = \frac{p_oR^2}{R^2 - 1}(1 + 2\,a/b) - \frac{2p_oR^2}{R^2 - 1} \quad (37)$$

From Equations 9 and 36, the stress concentration factor at the end of the minor axis is calculated to be

$$K_b = \frac{1 + 4\,b/a}{2} \quad (38)$$

and by Equations 9 and 37, the stress concentration factor at the end of the major axis is

$$K_a = 2\frac{a}{b} - 1 \quad (39)$$

To determine the limiting ellipse axis ratio it is necessary to equate the equivalent stresses, as given by Equation 28, at the ends of the two axes; thus,

$$(\sigma_o)_a^2 = (\sigma_o)_b^2 = (K_b\sigma_h)^2 + 2p(K_b\sigma_h) = (K_a\sigma_z)^2 + 2p(K_a\sigma_z) \quad (40)$$

For a closed-end cylinder, $\sigma_h = \sigma_z(R^2 + 1)$; therefore, by substituting this value of σ_h in Equation 40 along with values of K_b and K_a given by Equations 38 and 39, the limiting axis ratio, a/b, may be determined as a function of the wall ratio, R, as shown in Table VI.

If the ends of the cylinder are open, the longitudinal stress (Equation 11) becomes

$$\sigma_z = p_o \quad (41)$$

and Equations 36 and 27 become, respectively,

$$\sigma_h = \frac{2p_oR^2}{R^2 - 1}\left(1 + 2\,\frac{b}{a}\right) - p_o \quad (42)$$

and

$$\sigma_z = p_o(1 + 2\,a/b) - \frac{2p_oR^2}{R^2 - 1} \quad (43)$$

Similarly, Equations 38 and 39 become, respectively

$$K_b = (1 + 2\,b/a) - \frac{(R^2 - 1)}{2R^2} \quad (44)$$

and

$$K_a = (1 + 2\,a/b) - \frac{2R^2}{R^2 - 1} \quad (45)$$

Now, as before, by equating the equivalent stresses $(\sigma_o)_a$ and $(\sigma_o)_b$, it can be shown that there is no limiting axis ratio; in other words, for an open-end cylinder under internal pressure yielding will always initiate at the ends of the minor axis. The end condition of the cylinder has a large effect on the stress-concentrating effect of side holes, whereas in plain cylinders without side holes the effect is almost negligible.

Intermediate axis ratios between 1 and the critical values can be used to reduce stress concentration effects in cylinders. For many cylinders such ellipses can be obtained by tangential drilling of the side hole, using a cylindrical drill.

Table V. Elastic-Limit Pressures for Closed-End Cylinders

Wall Ratio, R	Relative Elastic Limit for Side Hole Ratios of ∞	5	1	Variable ($K = 6$)
2	1.00	0.447	0.473	0.210
3	1.185	0.560	0.575	0.285
4	1.250	0.605	0.625	0.296
9	1.315	0.645	0.670	0.322

Table VI. Limiting Values of Axis Ratio for Elliptic Side Hole in Closed-End Cylinder

Wall Ratio, R	Axis Ratio, a/b
1.5	2.57
2.0	3.28
2.5	4.09
3.0	5.00
3.5	6.02
4.0	7.13
5.0	9.68
10.0	29.21

Acknowledgment

Frank McClintock, Massachusetts Institute of Technology, suggested applying hydrostatic tension to the cylinder with a side hole, to make the problem amenable to analysis. The photoelastic work on circular side holes was performed by Miklos Hetenyi, Northwestern University. The authors acknowledge the assistance rendered by these men and extend thanks to Edward Saible, Carnegie Institute of Technology, who commented on many aspects of the work.

Literature Cited

(1) Am. Welding Society, Pressure Vessel Research Committee, Design Division, *Welding J.*, Research Supplement, January 1953.
(2) Faupel, J. H., *Trans. Am. Soc. Mech. Engrs.* **78**, 1031–64 (1956).
(3) Fessler, H., Lewin, B. H., *Brit. J. Appl. Phys.* **7**, 76–9 (1956).
(4) Lamble, J. H., Bayaumi, S. E. A., *Proc. Inst. Mech. Engrs.* **1B**, 575–9 (1952–53).
(5) Peterson, R. E., "Stress Concentration Design Factors," Wiley, New York, 1953.
(6) Schoessow, G. J., Kooistra, L. F., *Trans. Am. Soc. Mech. Engrs.* **12**, 107–12 (1945).
(7) Timoshenko, S., "Theory of Elasticity," McGraw-Hill, New York, 1934.
(8) Wang, C. T., "Applied Elasticity," McGraw-Hill, New York, 1953.

RECEIVED for review April 8, 1957
ACCEPTED September 5, 1957

Division of Industrial and Engineering Chemistry, High Pressure Symposium, 131st Meeting, ACS, Miami, Fla., April 1957.